International Journal of Pavement Research and Technology
https://doi.org/10.1007/s42947-023-00384-x

社團法人中華鋪面工程學會
Chinese Society of Pavement Engineering

ORIGINAL RESEARCH PAPER

Micro-mechanistic and Spectroscopic Analysis of RAP-Blended Asphalt Binders Rejuvenated with Waste Oils

Sumon Roy[1] · **Zahid Hossain**[2] · **Gaylon Baumgardner**[3] · **Musharraf Zaman**[4]

Received: 29 June 2023 / Revised: 10 September 2023 / Accepted: 15 September 2023
© The Author(s), under exclusive licence to Chinese Society of Pavement Engineering 2023

Abstract

In the United States, each year over 100 million tons of asphalt pavement material is reclaimed due to its multifold benefits. The use of reclaimed asphalt pavement (RAP) in preparing new asphalt concrete saves money, safeguards the environment, reduces waste in landfills, conserves other natural resources, and increases the durability and longevity of pavements. However, a high percentage of RAP in asphalt concrete can lead to developing premature failure of asphalt pavements due to fatigue cracking. On the other hand, the use of softening agents in asphalt binders can resolve these problems. To this end, two waste products, namely, waste cooking oil (WCO), and engine bottom oil (EBO) along with a commercial rejuvenator were evaluated in this study. The efficacy of these softening agents in aged asphalt binders has been investigated at micro- and macro-levels. Three types of Performance Grade (PG) binders, namely, PG 64-22, PG 70-22, and PG 76-22, each collected from two different sources, were blended with 25% RAP binders and different percentages (0%, 15%, and 20% by the weight of the binder blend) of the selected softening agents. Selected Superpave tests, the Atomic Force Microscopy (AFM)-based PeakForce Quantitative Nanomechanical Mapping (PFQNM™), and Fourier Transform Infrared Spectroscopy (FTIR) analyses were done on the unrejuvenated and rejuvenated binders. It was found that the rejuvenators improved the flow behavior of the RPA-modified binder samples. The AFM test results showed that the micro-level modulus and deformation values of rejuvenated binders were significantly less than those of their unrejuvenated counterparts. Similarly, distinct peaks were conformed in the FTIR peaks for EBO and WCO-modified binders. The EBO or WCO helped to reduce the RAP-blend binder's viscosity (e.g., lower mixing and compaction temperatures) and increase its rate of relaxation rates (e.g., improved thermal cracking resistance). Experimental data suggest that 10% EBO or WCO has similar beneficial effects in terms of improving 25% RAP-blended binders' fatigue and thermal cracking resistance compared to the commercial rejuvenator, whereas WCO was more effective in reducing stripping potential than EBO. The findings of this study will help pavement professionals in selecting suitable rejuvenators for the construction of pavements with high RAP contents.

Keywords Asphalt binder · Waste cooking oil · Engine bottom oil · Morphology · Modulus · Atomic force microscope

1 Introduction

In recent years, reclaimed asphalt pavement (RAP) has become an important source in the construction of hot mix asphalt (HMA) pavements in the United States (U.S.) and around the world. The binder extracted and recovered from the RAP materials is often known as reclaimed asphalt binder (RAB) [1]. According to a Federal Highway Administration (FHWA) study, more than 90% of roads and highways in the U.S. are constructed with the HMA [2]. Therefore, a huge amount of RAP is generated annually from the repairing of existing asphalt pavements and reconstruction of new pavements. The FHWA has highlighted using recycled materials in highway construction projects due to their engineering, economic, and environmental benefits [3, 4]. Thus, the use of RAP in the construction of asphalt pavement can become an important source of energy and cost savings [5].

However, the use of high RAP content in pavement construction is a major concern to transportation agencies to predict the performance of RAP-modified asphalt pavement during the design period. Based on the Arkansas Department of Transportation (ARDOT) Standard Specifications for Highway Construction, the contractors are restricted from using RAP in the job mixture where the mixture must contain a minimum of 70% virgin material. The ARDOT

Extended author information available on the last page of the article

Published online: 01 November 2023

has provisions to use RAP with some restrictions, which include that a softening agent along with the accompanying specifications should be submitted and approved before using it with the binders. A temperature-viscosity curve for the blending of RAP and virgin asphalt is required to be supplied by the contractors as well. Because of the limitations/restrictions in the ARDOT's current specifications, the brittle nature of RAB, lack of expertise in the processing of RAP, the variability of RAP among milling sources, lack of the availability of quality RAP, lack of prior experience, or a combination of any of these, the usage of more than 15% of RAP in the asphalt mixture is not generally practiced by the contractors. The contractors and agencies are very concerned about production temperatures, fatigue, and low-temperature performance of concrete with high RAP contents.

To improve the fatigue resistance of new asphalt mixtures with RAP, either a soft binder or a rejuvenating agent with a hard binder is commonly used [6]. Multiple researchers reported that rejuvenators can restore the original characteristics of the aged binder, which can be obtained from different materials, such as a soft binder, vegetable oils, waste engine oils (EBO), waste oil (frying oil), waste cooking oil (WCO), derived oils, as well as composite rejuvenator [7–15]. The United States Environmental Protection Agency (US EPA) has also estimated that about 380 million gallons of EBO are recycled each year, and it further states, "used oil from one oil change can contaminate one million gallons of fresh water—a years' supply for 50 people [16]." On the other hand, US hotels and restaurants generate about 3 billion gallons of WCO per year [17]. The generated EBO and WCO are mostly refined and reused as sources of furnace fuel oil, but this technique is not a sustainable practice. Thus, the use of EBO and WCO as rejuvenators will help reduce the environmental burden of society as well as reduce the construction material costs. To this end, two locally available waste oils, EBO and WCO, were selected in this study to examine their effectiveness in improving the fatigue resistance of asphalt mixtures blended with a higher RAP amount.

While macro- and micro-level properties of asphalt materials are commonly investigated, their molecular-level qualitative morphological and mechanistic data are indicators of long-term durability. Toward gathering molecular-level properties of asphalt binders, the Atomic Force Microscope (AFM) technique has been used by several researchers [18–27]. These researchers reported that the AFM technique can be used to investigate the surface microstructures as well as the micromechanical properties such as DMT (Derjaguin, Muller, and Toropov) modulus, adhesion, deformation, and energy dissipation of the asphalt binders. Moreover, these researchers described three distinct phases namely, dispersed phase (Catana), interstitial phase (Peri-phase), and matrix (Para-phase) to characterize the morphological clusters, which were also followed in the current study. Additionally, the Fourier transform infrared spectroscopy (FTIR) test was used on selected blended asphalt samples to detect the presence of any in the functional group due to the rejuvenation using softening agents [9, 28–30].

The major objectives of this study are to (1) observe the effectiveness of waste-based rejuvenators in asphalt binders, and (2) characterize atomic level morphological and mechanical properties of rejuvenated asphalt binders. To achieve the goal of this study, the AFM and FTIR tests were conducted to determine the molecular level properties. The Superpave tests were also included to compare the micro-level findings with the macro-level properties of rejuvenated binders. Therefore, this study aims to find a low-cost softening agent that can be used as a substitute for commercially produced rejuvenators to produce the desired asphalt mixtures containing high RAP contents.

2 Materials and Test Methods

2.1 Materials

2.1.1 Asphalt Binders, RAP Samples, and Softening Agents

Based on the Qualified Product List (QPL) of ARDOT, the following three types of Performance Grade (PG) asphalt binders were collected from two different sources: one PG 64-22 binder, two polymer-modified PG 70-22, and PG 76-22 binders. The first set of asphalt binders was prepared from a Canadian crude source. The second set of binders was made from an Arabian crude source, which is a combination of "sweet and sour crudes."

Two RAP samples were collected with the help of a local contractor in Jonesboro, AR, and they were investigated in this study. One RAP sample originated from a roadway section on Interstate 555 (I-555) between Marked Tree and I-55 while the other RAP sample was obtained from U.S Highway 67 (Hwy 67) between the Lawrence County line and Hwy 62 in Pocahontas, AR. The collected RAP samples were used for binder recovery in the laboratory. The recovered binders of different percentages were blended with the PG binders, and they were further blended with softening agents. Three RAP blends (0%, 15%, and 25% by weight) were prepared and tested in this study. However, this study presents test results of 25% RAP1 blends with a selective dose of the softening agents.

An engineered (i.e., commercially produced) rejuvenator, henceforth named EVF, was collected from its manufacturer's plant. Based on previous research findings, two waste-based softening agents, namely, WCO and EBO were collected from a local restaurant and an automobile dealer, respectively, in Jonesboro, AR. The WCO and EBO samples (each about 5 gallons) were no more than one day of

cumulative waste of soybean and motor (mostly SAE 10W-30) oils, respectively. Soybean oil is generally composed of five fatty acids: palmitic acid (~ 10%), stearic acid (~ 4%), oleic acid (~ 18%), linoleic acid (~ 55%), and linolenic acid (~ 13%). The EBO is a blend of base oils composed of petroleum-based hydrocarbons, polyalphaolefins, or their mixtures with a flashpoint of about 215 °C. A higher dosage level (15% or 20% by the weight of the binder) of the rejuvenators was not found to be effective based on preliminary test results as blended binders were highly soft. Thus, a 10% dosage level of the rejuvenator was explored further in this study. The dosages of WCO and EBO were selected as 10% (by weight of total binder blend) for the laboratory testing and evaluations. These dosage levels were chosen based on evidence from in-house laboratory data as well as recommendations from relevant studies available in the public domain. In this study, both WCO and EBO were used as-is conditions, without any improvements, processing, or modification, only after filtering coarse particles/substances to uniformly blend with the binders.

Table 1 summarizes the details of the asphalt binders, RAP, and rejuvenators used for this study. While naming the test samples, the following nomenclature was used: the binder source was followed by binder grade, which is followed by RAP No. and amount (%), which is followed by rejuvenator type and amount (%), and then lastly the aging condition (U for unaged, R for short-term aged, and P for long-term aged). For example, S1PG64-22 + RAP1(25) + EVF(10)U denotes the test sample is a Source 1 PG 64-22 binder with 25% RAP1 that is rejuvenated with 10% EVF and the binder is unaged.

2.1.2 Blending of Asphalt Binders

A blending protocol, originally developed in 2013 by Hossain et al. [31], for mixing RAP binder along with additives and virgin binder in the laboratory was followed in this study. In a recent relevant study of the current research team, the same blending protocol was also used to examine some of the morphological and nanomechanical properties of selected rejuvenated asphalt binders containing high RAP binders [32]. The major steps involved in the blending of asphalt binders used in this study are given below:

- Firstly, a neat binder was heated in the aluminum can at 160 °C for nearly 20 min (mins) to make it workable.
- The container of the RAP binder was heated separately at the same time. The required amount of RAP binder was poured into the base binder container.
- The container of RAP and neat binder were kept in the oven at 160 °C for nine mins.
- A glass rod was used for stirring the mixture for 1 min vigorously and uninterruptedly.

Table 1 Details of asphalt binders, RAPs, and rejuvenators

Asphalt binders				
Crude source	Asphalt binders	Modifiers	Flash point (°C)	Viscosity at 135 °C (mPa s)
Canadian (Source 1; S1)	PG 64-22	None	318.00	390
	PG 70-22	Polymer	312.78	1180
	PG 76-22	Polymer	322.78	1580
Arabian (Source 2; S2)	PG 64-22	None	356.00	474
	PG 70-22	Polymer	342.00	954
	PG 76-22	Polymer	320.00	1779

Reclaimed asphalt pavements (RAPs)		
RAP type	Amount of RAP (% by wt)	Origin/collection source
RAP1	0%, 15%, and 25%	I-555; between Marked Tree and I-55, AR
RAP2	0%, 15%, and 25%	Hwy 67; between the Lawrence County line and the Hwy 62 in Pocahontas, AR

Softening agents		
Agent type	Dosage (%) (wt of the total binder)	Origin/collection source
WCO	10%, 15%, and 20%	Local Restaurant, Jonesboro, AR
EBO	10%, 15%, and 20%	Automobile Dealer, Jonesboro, AR
EVF	10%, 15%, and 20%	Commercial Lab

- The mixture was then kept in the oven for heating for another 9 min and 1 min of stirring.
- This cycle (heating for 9 min and stirring for 1 min) was repeated a total of six times allowing sixty minutes (1 h) of blending time for every mixing type.
- During the blending process, the interior wall of the sample container was scrapped periodically to prevent the accumulation of RAP binders on the sides of the container.
- To prepare the rejuvenated RAP blends, the required amount of softening agent (e.g., WCO, EBO, and EVF) was added into the container of the base binder along with the RAP binder before starting the "heating and stirring" cycle.
- In the end, the blended asphalt binder was then allowed to cool down to room temperature and stored for further testing.

2.2 Test Methods

2.2.1 Rotational Viscosity (RV) Test

The RV tests were done on rejuvenated asphalt binders to measure the workability, pumpability, and mixability of the asphalt binders at high manufacturing and construction temperatures. In this study, the RV test was performed as per AASHTO T 316 in the laboratory using a DV-II + Pro rotational viscometer (RV), as shown in Fig. 1a. The RV test was performed to measure the viscosity of rejuvenated asphalt binders at a temperature of 135 °C up to 180 °C at an interval of 15 °C. A total of three replicates were used to measure the viscosity of the binders and their average values were then used in this study.

2.2.2 Dynamic Shear Rheometer (DSR) Test

In this study, the dynamic shear rheometer (DSR) test was conducted to characterize the viscous and elastic behavior of rejuvenated binders at high and intermediate service temperatures. In the DSR test, the asphalt binder sample is sandwiched between a fixed plate and an oscillating plate. The DSR tests were performed at a frequency of 10 radians per second (1.59 Hz) per AASHTO T 315 where a 1.00 mm gap between was used for 25-mm parallel plates. The DSR machine used in this study is shown in Fig. 1b. To ascertain the repeatability of test data, three replicate specimens were tested for each test condition.

2.2.3 Bending Beam Rheometer (BBR) Test

The BBR test was done to find the low-temperature properties of the PAV-aged rejuvenated binders to determine their creep stiffness (S-value) and the slope of the master stiffness curve (m-value). This test was performed per AASHTO T 313 at a temperature of −9 °C and −12 °C. In this test, the "*m*-value" at 60 s of load and the S-value at 60 s (MPa) were determined for binder samples. The BBR tests were conducted at a lab located at the University of Oklahoma in Norman, Oklahoma. At least two replicate specimens were at each test temperature to ascertain the repeatability of test data in the laboratory. The BBR device used in this study is shown in Fig. 1c.

2.2.4 Atomic Force Microscope (AFM) Tests

In recent years, the Atomic Force Microscope (AFM) has been used by multiple researchers to determine the properties of asphalt binders at a microscale. It is found that the AFM is a useful tool to observe the microstructures presented on the asphalt binder surface and quantify the mechanical properties by correlating its morphological

(a) (b) (c)

Fig. 1 Superpave devices used in this study: **a** rotational viscometer (RV), **b** dynamic shear rheometer (DSR), and **c** bending beam rheometer (BBR)

properties. In this study, the Dimension Icon AFM from Bruker has been used to observe the binders' surface roughness and its mechanical properties such as the DMT (Derjaguin, Muller, and Toropov) modulus, and deformation at the nanoscale. The PeakForce Quantitative Nanomechanical Mapping (PFQNM™) mode of the AFM system was used as it provides maps for the surface roughness and mechanistic properties simultaneously at a molecular level. Similar to the tapping mode, the peak force tapping provides the surface morphology and the force–displacement curve of any point under the scan area which are analyzed through the quantitative nanomechanical mapping to find the properties of the scanned surface.

The heat cast approach is used by several researchers in the characterization of asphalt binders, which was also used in this research to prepare the AFM test specimens [18–27, 32–37]. Firstly, the asphalt binder sample was heated in a preheated oven at 160 °C until it became sufficiently fluid to pour. Then, a very small amount of asphalt binder, generally 2 drops, was placed on a thin glass plate (size: 50 mm × 75 mm). The binder sample with the glass plate was then placed in the oven for approximately 15–20 min to obtain a smooth surface of the binder. Before testing, the prepared specimens were cooled at room temperature for 30 min in the air and later, stored in a humidity-controlled desiccator for 24 h. In this study, three replicated samples were prepared and tested for each binder type. Afterward, the scanned maps were analyzed offline using the NanoScope (version 9.0) software to quantify the roughness and mechanical properties of rejuvenated asphalt binders.

In the AFM test, stiff probes (RTESPA™) were employed to determine the mechanistic properties of modified asphalts. The tips were calibrated for exact values of deflection sensitivity, spring constant (k), and tip-end radius before scanning the binders. The length, width, drive frequency, and quality factor of the AFM probe were 120 µm, 40.5 µm, 299.5 kHz, and 292, respectively. The normal constant for the tip was calculated as 25.6 N/m using the Sader method. After the calibration, the accuracy of the AFM system with the calibrated tip was verified by testing a standard Polystyrene-Low Density Polyethylene (PS-LDPE) sample. The size of the scan area was chosen as 30 µm × 30 µm. The PeakForce Tapping frequency of 1 kHz was used in the AFM tests where the PeakForce engagement amplitude and setpoints were selected as 150 nm and 0.05 V, respectively.

2.2.5 Fourier Transform Infrared Spectroscopy (FTIR) Test

The FTIR test is a spectroscopy test performed on unmodified and modified asphalt samples to detect the presence of any in the functional group due to any modification using RAPs and rejuvenation using softening agents. In this study, disposable Real Crystal IR cards, containing a KBr substrate were used for the sample preparation. A blank card was scanned before starting the test and it was repeated every 1-h interval. A Nicolet 8700 spectrometer was used in this study. To prepare the sample, the rejuvenated binder sample was heated at a temperature of 163 °C until it became sufficiently fluid and workable. A small amount (e.g., 1–2 drops) of hot asphalt binder was dropped right outside the aperture and dragged over the KBr substrate to make the coating of the sample on the KBr plate. The aperture of the hole in the plate was 15 mm. A spectrum range of 450–4000 cm^{-1} was used in this study. The samples were run over 50 scans at 4 cm^{-1} resolutions for 30 s. The test was conducted at a relative humidity of under 5%. Finally, the test data were analyzed using Omnic 6.2 software.

2.2.6 Texas Boiling Test (TBT)

To evaluate the performance of rejuvenated binders against the moisture damage potential, a relatively simple and quick method, namely, the Texas Boiling Test (TBT), was included in this study. In the TBT test, the stripping of the asphalt mixtures was predicted based on visual observation after 10 min of boiling the asphalt mixtures in hot water. The TBT was done per ASTM D3625. The percentage of asphalt binder based on the binder's retention on the surface of the mineral aggregates after boiling was determined by following the guidelines established by the Texas Transportation Institute (TTI). In the TBT, limestone aggregates, collected from a local quarry, that passed a 9.5 mm (3/8″) sieve and retained on an ASTM No. 4 Sieve were used in this study. The limestone aggregates were selected for this study as they exhibited a higher moisture damage resistance compared to dolomite, sandstone, and gravel [18, 19, 35].

3 Results and Discussion

3.1 RV Tests

The RV tests were conducted on unrejuvenated and rejuvenated RAP blends, as shown in Fig. 2. In the RV tests, a total of three replicate specimens were tested for each test temperature of 135 °C, 150 °C, 165 °C, and 180 °C. For each specimen, three viscosity readings were recorded at 1-min intervals at each test temperature, and the average values were taken into consideration for data interpretation. RV test results showed that the viscosity data of RAP1 is very comparable with that of RAP2 even though their sources and histories are different from each other. It is also observed that higher dosages (e.g., 15 or 20%) of the softening agents are not beneficial. Further, previous literature review data suggest that 10% (by the weight of the binder blend) is optimum. Thus, RV test data of RAP1

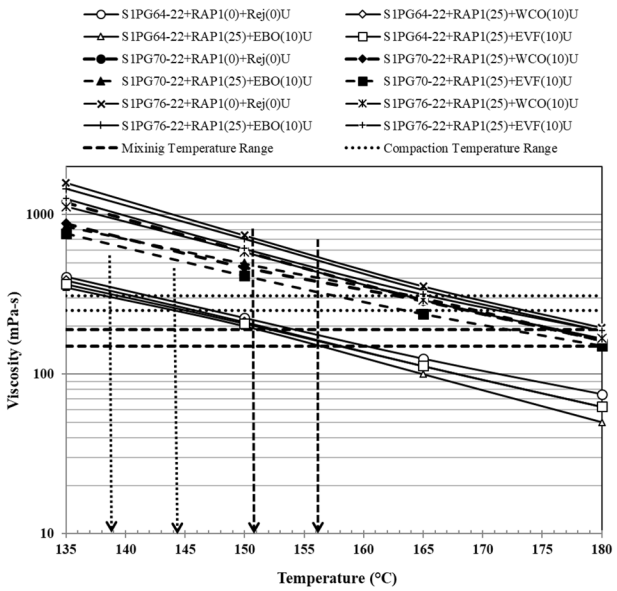

Fig. 2 Comparison of viscosities of rejuvenated binders

blends (0, 15, and 25 by the weight of the total binder) of all three binders (PG 64-22, PG 70-22, and PG 76-22) from both sources (S1 and S2) with 0% (Control) and 10% softening agents have been evaluated and explained thoroughly in this paper.

As seen in Fig. 2, the rejuvenators decreased the viscosity of all binder blends irrespective of the binder grade and test temperature. It is also evident that the reduction of the viscosity values of 25% RAP1 blends followed a similar trend in the cases of WCO and EVF rejuvenators compared to EBO, which showed the most reduction of viscosity values. The reduction of viscosities is expected to facilitate lower production temperatures (mixing and compaction) for rejuvenated asphalt binder mixes compared to their unrejuvenated counterparts.

The mixing and compaction temperatures for all rejuvenated blends are presented in the form of dash lines in Fig. 2. The mixing and compaction temperatures of HMA are expressed in ranges of temperature based on the viscosities of asphalt binders as per AASHTO T 312 Standard [38]. The viscosity values of 170 ± 20 mPa-s and 280 ± 30 mPa-s are recommended for determining the mixing and compaction temperature, respectively. In this study, the mixing and compaction temperatures of the binder blends are calculated as per ASTM D 2493 [39]. The addition of the rejuvenators reduced the viscosities at each tested temperature in all binders containing 25% of RAP than their corresponding unrejuvenated binders. For instance, a mixing temperature range of 152–158 °C was found for a rejuvenated 25% RAP blend with a 10% EVF with PG 64-22 as designated as S1PG64-22 + RAP1(25) + EVF(10)U in Fig. 2. The compaction temperature range of this binder blend was found to be in the range of 140–146 °C. Therefore, it can be said that this rejuvenated blend can be mixed at 155 °C ± 3 °C and compacted at 143 °C ± 3 °C that contains 25% of RAP binder. On the other hand, the mixing and compaction temperatures of the corresponding unrejuvenated binder, i.e., S1PG64-22 + RAP1(25) + Rej(0)U are 157 °C ± 3 °C and 145 °C ± 3 °C, respectively. Thus, the reductions of mixing and compaction temperatures of the EVF-rejuvenated PG 64-22 binder with 20% RAP binder are about 2 ± 2 °C and 2 °C, respectively. The mixing and compaction temperatures of all rejuvenated binders from S1 are summarized in Table 2.

Table 2 represents the summary of the RV test results of the asphalt binders. It is seen that all S1 binders exhibit significantly higher viscosity values compared to the corresponding unmodified or modified binders from S2,

Table 2 Mixing and compaction temperatures of S1 rejuvenated binders

Base binder type	Sample description	Mixing temperature (°C)		Compaction temperature (°C)	
		Low	High	Low	High
PG 64-22	S1PG64-22 + RAP1(0) + Rej(0)U	154	160	142	148
	S1PG64-22 + RAP1(25) + WCO(10)U	152	158	140	145
	S1PG64-22 + RAP1(25) + EBO(10)U	151	156	139	144
	S1PG64-22 + RAP1(25) + EVF(10)U	152	158	140	146
PG 70-22	S1PG70-22 + RAP1(0) + Rej(0)U	176	182	164	179
	S1PG70-22 + RAP1(25) + WCO(10)U	174	180	161	167
	S1PG70-22 + RAP1(25) + EBO(10)U	173	180	159	165
	S1PG70-22 + RAP1(25) + EVF(10)U	172	179	158	164
PG 76-22	S1PG76-22 + RAP1(0) + Rej(0)U	181	187	168	174
	S1PG76-22 + RAP1(25) + WCO(10)U	176	182	164	169
	S1PG76-22 + RAP1(25) + EBO(10)U	177	183	156	171
	S1PG76-22 + RAP1(25) + EVF(10)U	174	184	161	167

indicating that S1 binders were relatively stiffer than S2. Also, as expected, the base binder (PG 64-22) exhibited the lowest viscosity among all unaged binders irrespective of its source. Table 2 also shows the aging indices for comparing the aging effect in the viscosity of the same asphalt binder at two aging conditions (e.g., unaged and RFTO aged). To obtain an aging index, the viscosity of an asphalt binder sample was divided by the corresponding viscosity of the unaged counterpart. For example, in the case of the S1B1 binder, the aging index for the RTFO-aged binder was found to be 2.4, which was calculated by dividing 1229 mPa s with 504 mPa s. It is noted that PPA plus SBS modified PG 76-22 binders from both sources showed the highest aging index value of 2.8 at 135 °C. A binder with a relatively high aging index indicates its high potential to become brittle and exhibit fatigue and low-temperature cracks in the pavement.

3.2 DSR Tests

Figure 3 shows the effects of rejuvenators on all RAP binder blends in the PG temperatures. It is found that the rejuvenated RAP blends became softer than their corresponding unmodified binder, and therefore, failed earlier in high temperatures. For example, the high PG temperature was found to be reduced from 82 to 76 °C for the PG 76-22 binder blends. The DSR test results show that the high PG temperature corresponding to the Superpave rutting factor of rejuvenated RAP blends of PG 64-22, PG 70-22, and PG 76-22 binders range from 61 to 64 °C, from 76 to 73 °C, and from

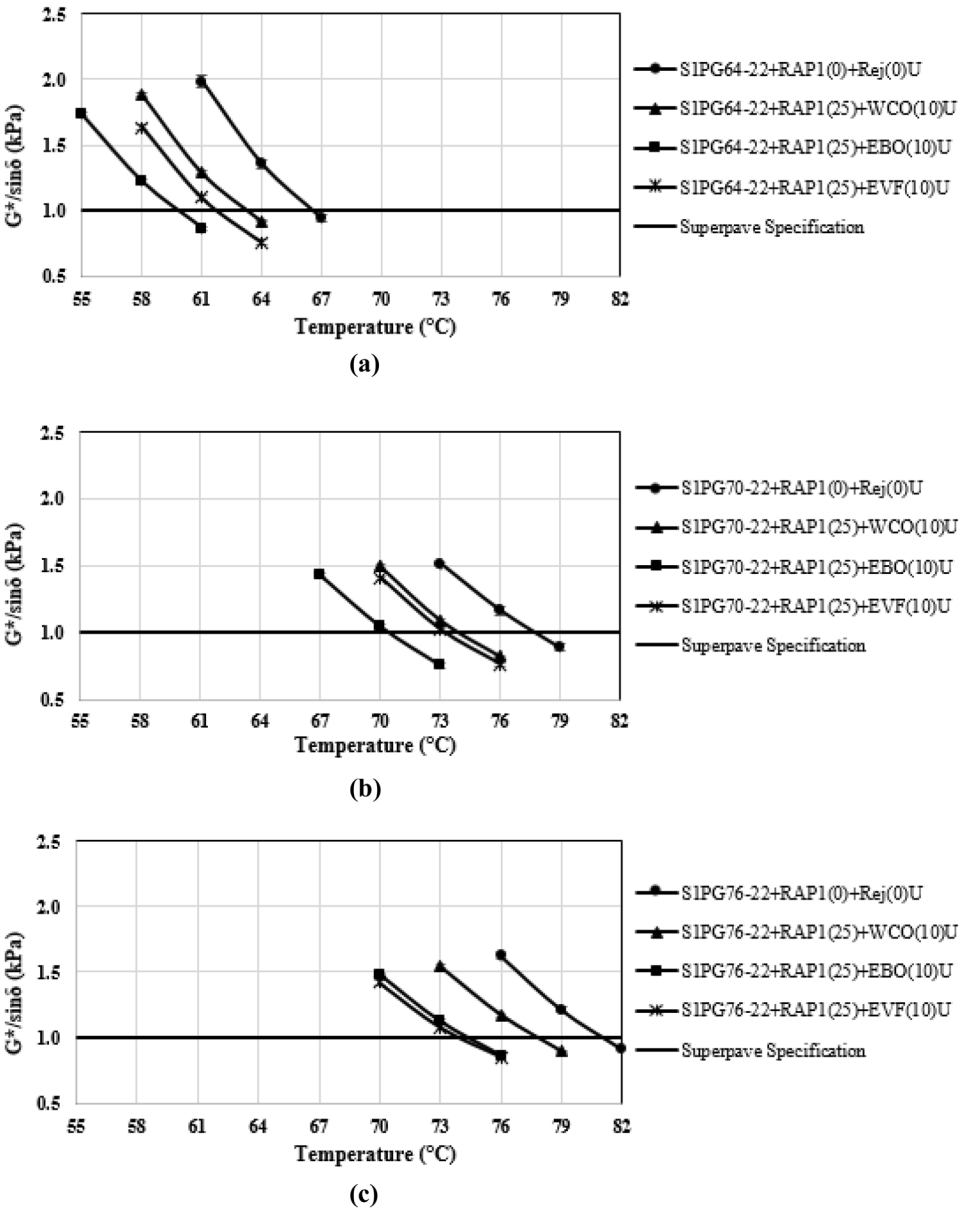

Fig. 3 DSR test results of rejuvenated base asphalt binders from S1: **a** PG 64-22, **b** PG 70-22, and **c** PG 76-22

79 to 76 °C, respectively. It is seen that the EBO-modified RAP blends exhibited lower failure temperatures compared to WCO and EVF among all binders. Generally, the range of high PG temperature of rejuvenated blends containing 25% RAP binders is slightly lower than that of the unrejuvenated counterparts. Thus, it can be said the rejuvenators acted as the binder softeners for all RAP blends. It is also expected that the low PG temperatures of these RAP blends would also be somewhat lower, which will be discussed in a later section.

3.3 BBR Tests

The BBR test was conducted to measure the low-temperature stiffness and cracking properties of rejuvenated asphalt binders (Fig. 4). In this study, the BBR test was done for the PG 64-22, PG 70-22, and PG 70-22 binder samples from S1 modified with 25% of RAP1 binder contents and all three rejuvenators (i.e., WCO, EBO, and EVF). For all tested binder samples, the measured creep stiffness and m-value at the 60 s at − 9 °C and − 12 °C are shown in Fig. 4.

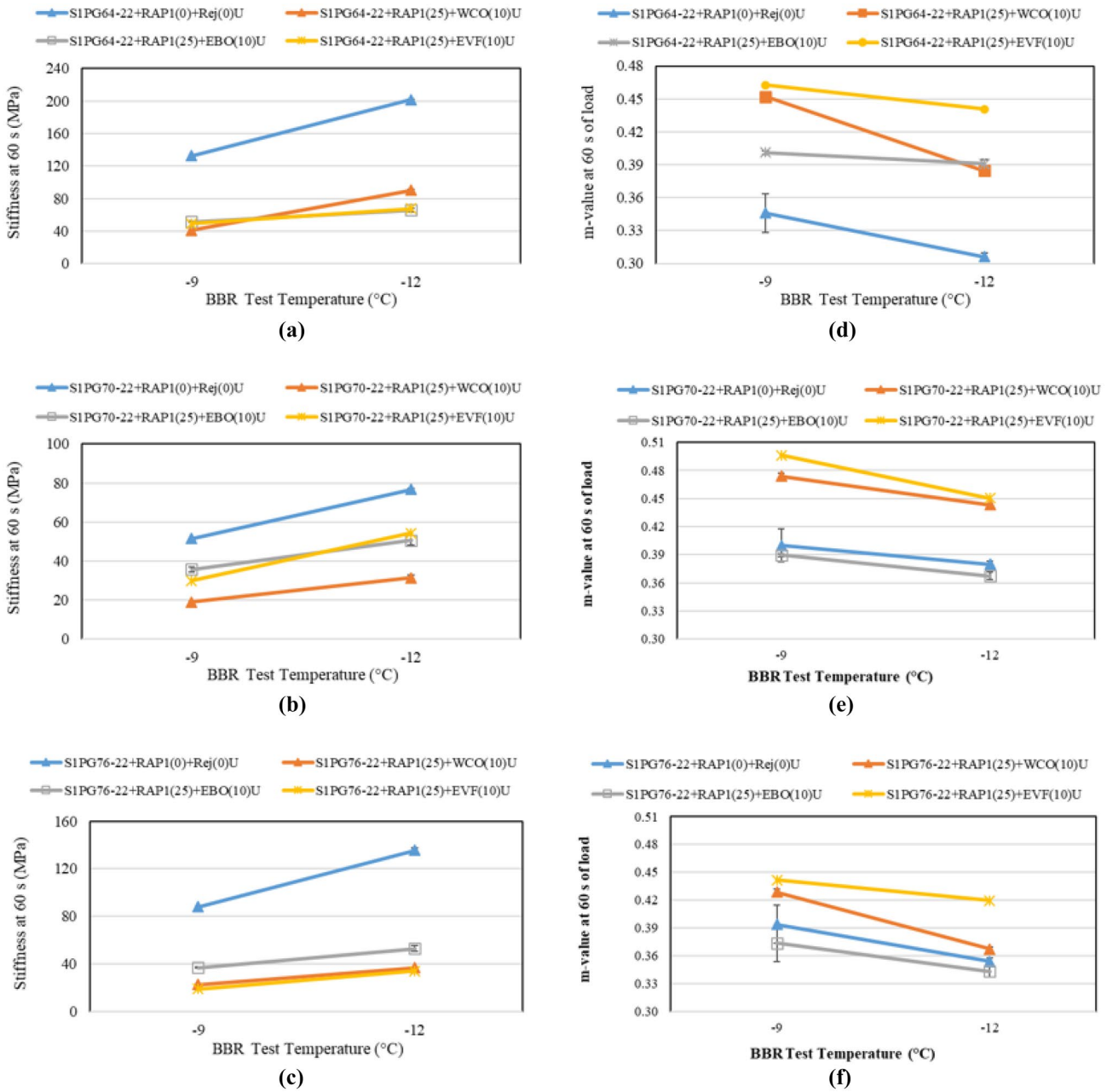

Fig. 4 "m-values" and creep stiffness of rejuvenated binders from S1

As seen in Fig. 4, the stiffness values at 60 s were increased at the testing temperature from − 9 to − 12 °C for all rejuvenated and unrejuvenated binder blends. It is seen that rejuvenated binders showed a significant reduction in stiffness due to the rejuvenation compared to their corresponding unmodified binders. At − 9 °C, the RAP blends rejuvenated with EBO showed higher stiffness values compared to EVF and WCO-modified blends. As expected, the stiffness values of all rejuvenated asphalt binders increased with a decrease in the testing temperature, but they were well below the Superpave acceptance criteria of 300 MPa at a BBR testing temperature of − 12 °C (i.e., low PG temperature of − 22 °C).

Figure 4 also shows that the "m-values" of most of the samples were found to be reduced with a reduction of test temperature (i.e., from − 9 to − 12 °C), which was expected. It was observed that the EBO-modified binders exhibited the lowest "*m*-values" at 60 s of load in the case of PG 70-22 and PG 76-22 rejuvenated binders. Thus, the major finding from the BBR test results is that the softening agents increased the "*m*-value" (rate of stress relaxation) of RAP-blended binders indicating their beneficial effects. From the "*m*-value" perspective, EVF and WCO were found to outperform EBO. However, at a testing temperature of − 12 °C, all tested rejuvenated RAP-blended binders comfortably met the Superpave criterion for the rate of stress relaxation (*m*-value ≥ 0.300).

3.4 AFM Tests

Figure 5 represents the surface roughness of rejuvenated PG 76-22 binders. The effect of rejuvenators is seen in the

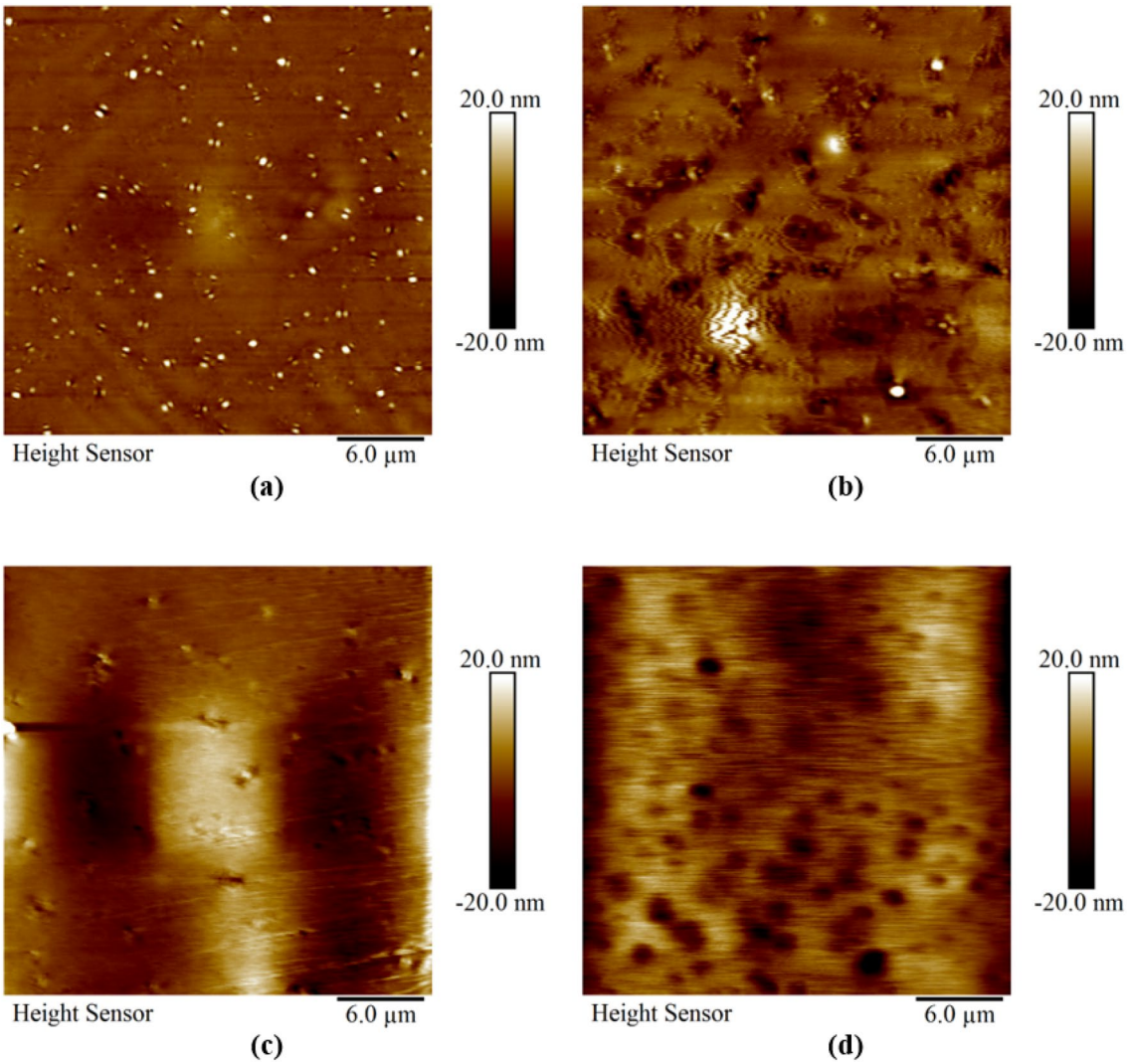

Fig. 5 Surface roughness of rejuvenated PG 76-22 S1 binders: **a** S1PG76-22 + RAP1(0) + Rej(0)U (unmodified); **b** S1PG76-22 + RAP1(25) + WCO(10)U; **c** S1PG76-22 + RAP1(25) + EBO(10)U; **d** S1PG76-22 + RAP1(25) + EVF(10)U

binder's surface morphology by observing the microstructural features (e.g., "bee structures"). The DMT Modulus and the deformation of rejuvenated PG 76-22 and PG 70-22 binders are shown in Figs. 6 and 7, respectively.

Table 3 shows the details of microstructural properties such as roughness, the number of phases observed, dominant phase, the appearance of the dispersed phase, wrinkling (dispersed phase), development of new phase, microstructure recovery, the shape of bees, etc. of rejuvenated PG 70-22 and PG 76-22 binders. From Table 3, it is seen that three distinct phases namely, (i) dispersed phase or Catana/bee structure), (ii) interstitial phase or peri phase, and (iii) matrix or para phase were presented in control binders. However, the addition of rejuvenators may eliminate these phases and create a new phase on the binder surface. For example, phases (i) and (ii) were found to disappear in the case of EVF-modified binders, and a new phase consisting of black dots/spots, a circular-shaped phase was developed. As a result, the wrinkling pattern on the binder surface was missing due to the rejuvenation using the EVF. In most rejuvenated binders, the dispersed phase was found to be dominant with an appearance of well-dispersed along with some clustering. The shapes of the bees were found to be either elliptical or, irregular and conical hill-shaped for control, WCO- and EBO-modified rejuvenated binders while circular-shaped black spots were observed in the case of EVF-modified binders. Moreover, the surface roughness values were found to be lower in the rejuvenated binders compared to corresponding control binders except for EVF-modified binders. It is also found that the WCO- and EBO-rejuvenated binders exhibited better performance in terms of microstructure recovery than the EVF, which is also seen in Fig. 5.

Table 4 represents the quantitative details of observed microstructures (bees) in all rejuvenated binders from S1.

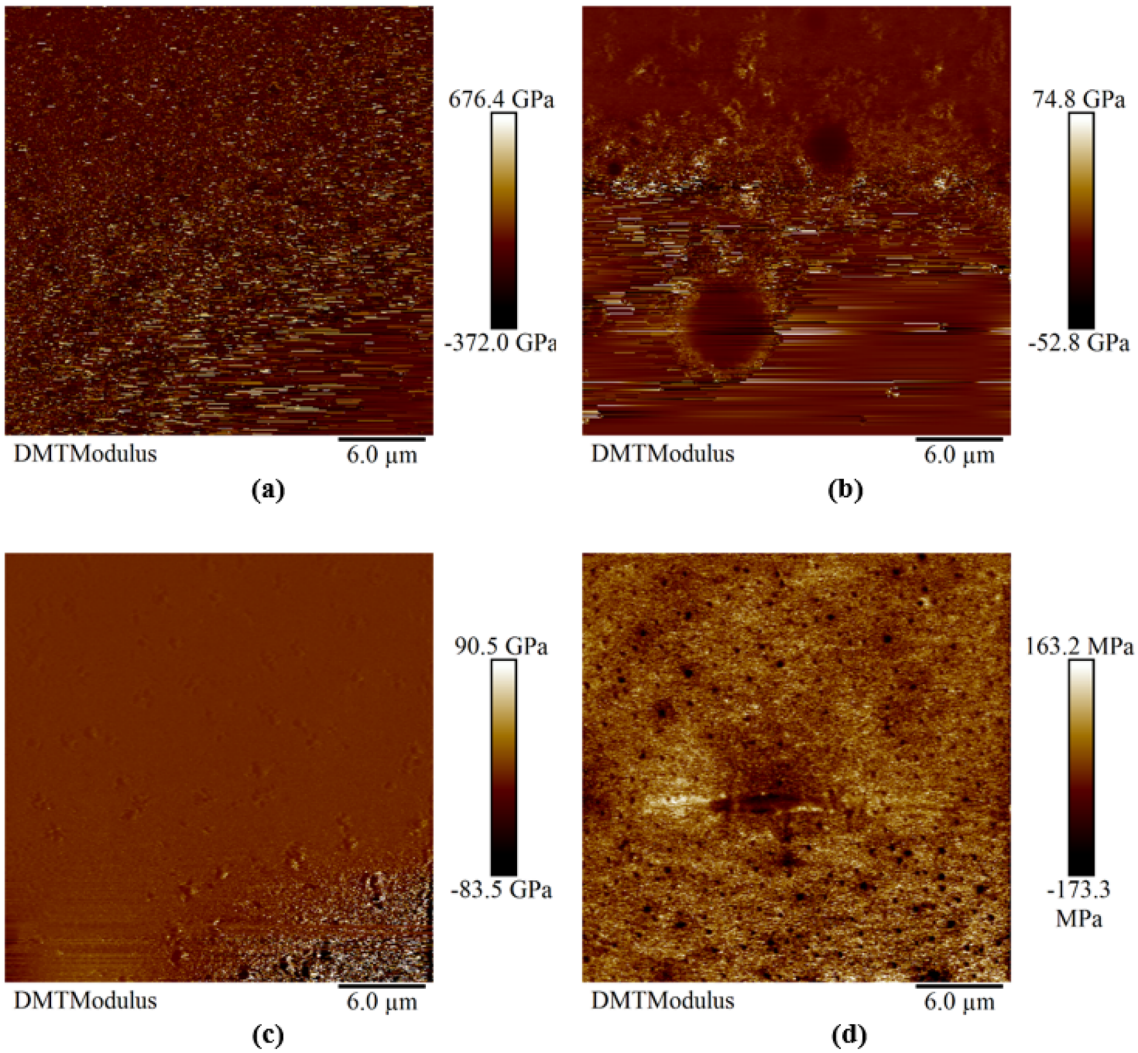

Fig. 6 DMT modulus of rejuvenated PG 70-22 S1 binders: **a** S1PG70-22+RAP1(0)+Rej(0)U (unmodified); **b** S1PG70-22+RAP1(25)+WCO(10)U; **c** S1PG70-22+RAP1(25)+EBO(10)U; **d** S1PG70-22+RAP1(25)+EVF(10)U

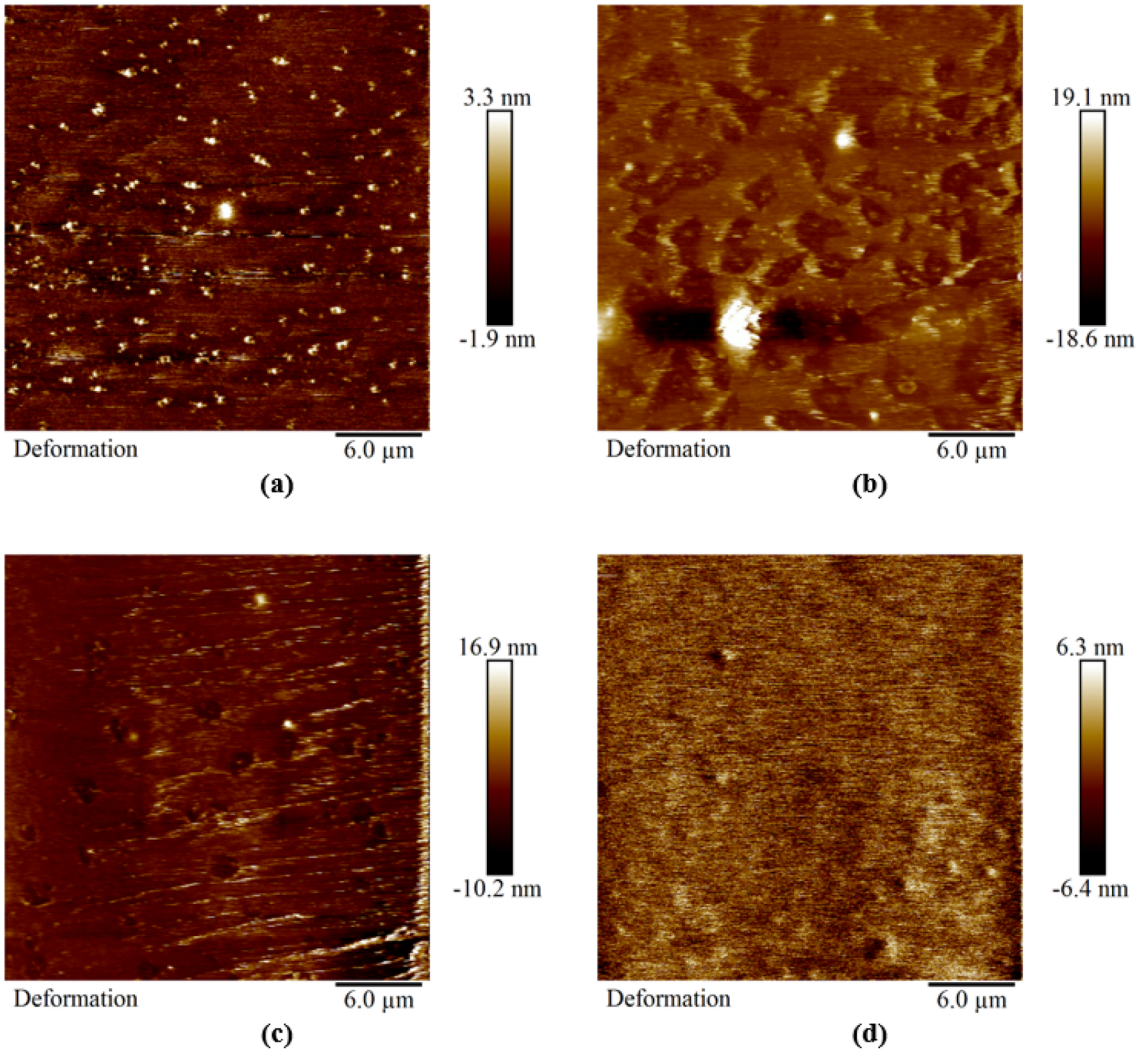

Fig. 7 Deformation of rejuvenated PG 76-22 S1 binders: **a** S1PG76-22+RAP1(0)+Rej(0)U (unmodified); **b** S1PG76-22+RAP1(25)+WCO(10)U; **c** S1PG76-22+RAP1(25)+EBO(10)U; **d** S1PG76-22+RAP1(25)+EVF(10)U

From Table 4, it is found that the size of bees (e.g., length (um) and width (um)) was significantly affected in the rejuvenated binders. For instance, the length and width of the bees were increased noticeably for rejuvenated PG 64-22 binders, from 1.90 to 3.59 um and from 0.84 to 1.99 um, respectively, for WCO-modified binders. A similar increasing pattern is noticed in the case of EBO and EVF-modified binders as well. This trend is also found for rejuvenated PG 70-22 and PG 76 binders, as excepted for EVF-containing binder blends, which were discussed in the previous section.

From Table 5, it is seen that the average modulus value for the control PG 76-22 binder was 521 MPa, and it varied from 510 to 610 MPa in the dispersed and interstitial phases, whereas it was found to range from 450 to 536 MPa in the recessed areas (matrix phase). With the increment of RAP percentage, the binder blend typically provides higher modulus values than the control binder and it makes the binder stiffer. However, as seen in Table 5, 25% of RAP blends did not show any increment of modulus values due to the rejuvenation of the blends using WCO, EBO, and EVF, resulting in lower modulus values. Although the decreasing trend was different for each rejuvenator, the least modulus value was found for EVF while WCO had the maximum modulus and EBO had an intermediate modulus between these two rejuvenators irrespective of the binder grades.

As seen in Table 5, the average values of deformation for the control PG 76-22 binder were found to be 5.0 nm over the scan area. The deformation values of the rejuvenated RAP blends were reduced in all cases. A deformation value of 2.80 nm, 2.93 nm, and 2.99 nm was observed for the WCO-, EBO-, and EVF-modified binder, respectively. However, the deformation of the binders was found to be higher if the corresponding modulus was lower due to the incorporation of rejuvenators.

Table 3 Qualitative microstructural properties of S1 rejuvenated binders

Microstructural features	S1PG70-22+RAP1(0)+Rej(0)U	S1PG70-22+RAP1(25)+WCO(10)U	S1PG70-22+RAP1(25)+EBO(10)U	S1PG70-22+RAP1(25)+EVF(10)U	S1PG76-22+RAP1(0)+Rej(0)U	S1PG76-22+RAP1(25)+WCO(10)U	S1PG76-22+RAP1(25)+EBO(10)U	S1PG76-22+RAP1(25)+EVF(10)U
Roughness (Rq) (nm)	2.29	1.99	1.59	4.3	2.27	3.92	2.48	5.73
Number of phases* observed	3(i+ii+iii)	2(i+iii)	3(i+ii+iii)	2(iii+iv)	3(i+ii+iii)	3(i+ii+iii)	3(i+ii+iii)	2(iii+iv)
Dominant Phase	Dispersed phase	Matrix phase	Dispersed phase	Matrix phase	Dispersed phase	Dispersed phase	Dispersed phase	Matrix phase
Appearance of Dispersed Phase	Well dispersed, some clustering	Well dispersed, some clustering	Well dispersed, some clustering	Not present	Well dispersed, some clustering	Well dispersed	Well dispersed	Not present
Wrinkling (Dispersed Phase)	Present	Present	Present	No	Present	Present	Present	No
Development of New Phase	No	No	No	(iv)	No	No	No	(iv)
Microstructure Recovery	Control	Yes	Yes	No	Control	Yes	Yes	No
Shape of bees	Elliptical	Irregular hill-shaped	Elliptical	Circular	Elliptical	Conical hill-shaped	Elliptical	Circular

*i) Dispersed phase (Catana/bee structure); ii) interstitial phase (peri phase); iii) Matrix (para phase) and iv) new phase (i.e., blackspot, circular-shaped phase)

Table 4 Quantitative details of observed microstructures (bees) in rejuvenated binders

Binder type	Length/Dia. (um)			Width (um)		
	Max	Min	Avg	Max	Min	Avg
PG 64-22						
S1PG64-22 + RAP1(0) + Rej(0)U	2.51	0.35	1.9	1.4	0.42	0.84
S1PG64-22 + RAP1(25) + WCO(10)U	6	2	3.59	3.01	1.25	1.99
S1PG64-22 + RAP1(25) + EBO(10)U	4.14	1.61	2.58	1.81	0.75	1.25
S1PG64-22 + RAP1(25) + EVF(10)U	5.85	1.89	3.6	3.05	1.16	2.16
PG 70-22						
S1PG70-22 + RAP1(0) + Rej(0)U	1.93	0.91	1.41	1.06	0.71	0.91
S1PG70-22 + RAP1(25) + WCO(10)U	1.81	0.93	1.48	0.97	0.3	0.57
S1PG70-22 + RAP1(25) + EBO(10)U	2.9	0.92	2.19	1.31	0.52	1.02
S1PG70-22 + RAP1(25) + EVF(10)U	1.79	0.6	1.13	–	–	–
PG 76-22						
S1PG76-22 + RAP1(0) + Rej(0)U	2.16	0.67	1.38	1.28	0.65	0.92
S1PG76-22 + RAP1(25) + WCO(10)U	4.48	2.35	3.07	4.48	2.35	3.07
S1PG76-22 + RAP1(25) + EBO(10)U	4.15	1.27	2.6	2.02	1.24	1.69
S1PG76-22 + RAP1(25) + EVF(10)U	2.2	0.87	1.5	–	–	–

Table 5 Mechanical properties of the rejuvenated binder blends

Binder description	Aging condition	Average DMT modulus (MPa)	Average deformation (nm)
PG 64-22			
S1PG64-22 + RAP1(0) + Rej(0)U	Unaged	132	11.10
S1PG64-22 + RAP1(25) + WCO(10)U	Unaged	105	3.77
S1PG64-22 + RAP1(25) + EBO(10)U	Unaged	93	4.60
S1PG64-22 + RAP1(25) + EVF(10)U	Unaged	77	7.15
PG 70-22			
S1PG70-22 + RAP1(0) + Rej(0)U	Unaged	390	5.97
S1PG70-22 + RAP1(25) + WCO(10)U	Unaged	254	2.71
S1PG70-22 + RAP1(25) + EBO(10)U	Unaged	205	1.28
S1PG70-22 + RAP1(25) + EVF(10)U	Unaged	193	2.04
PG 76-22			
S1PG76-22 + RAP1(0) + Rej(0)U	Unaged	521	5.0
S1PG76-22 + RAP1(25) + WCO(10)U	Unaged	406	2.80
S1PG76-22 + RAP1(25) + EBO(10)U	Unaged	366	2.93
S1PG76-22 + RAP1(25) + EVF(10)U	Unaged	327	2.99

The statistical analysis of AFM test data using ANOVA of Minitab 20 software showed that the p-values are less than the significance level ($\alpha < 0.05$) which indicates that the means of binder types, microscopic properties, and the interaction between binder type and microscopic properties are statistically significant. The interaction effect plot indicates that microscopic properties depend on the binders' PG.

3.5 FTIR Tests

The FTIR tests were conducted on unaged rejuvenated binder samples from S1 and S2, shown in Fig. 8a, b, respectively. Figure 9 shows the FTIR spectra of WCO and EBO before using them in RAP binder blends. It was found that the peak at certain wavenumbers displayed a higher signal, which indicated that the rejuvenations had introduced some increase in certain quantities in the rejuvenated binder samples.

The changes in the quantities of functional groups of asphalt binders before and after rejuvenation were estimated using the carbonyl (C=O), sulfoxide (S=O) peaks, and the Trans-Butadiene index (I_{SBS}). The values of the carbonyl index ($I_{C=O}$), the sulfoxide index ($I_{S=O}$), and the

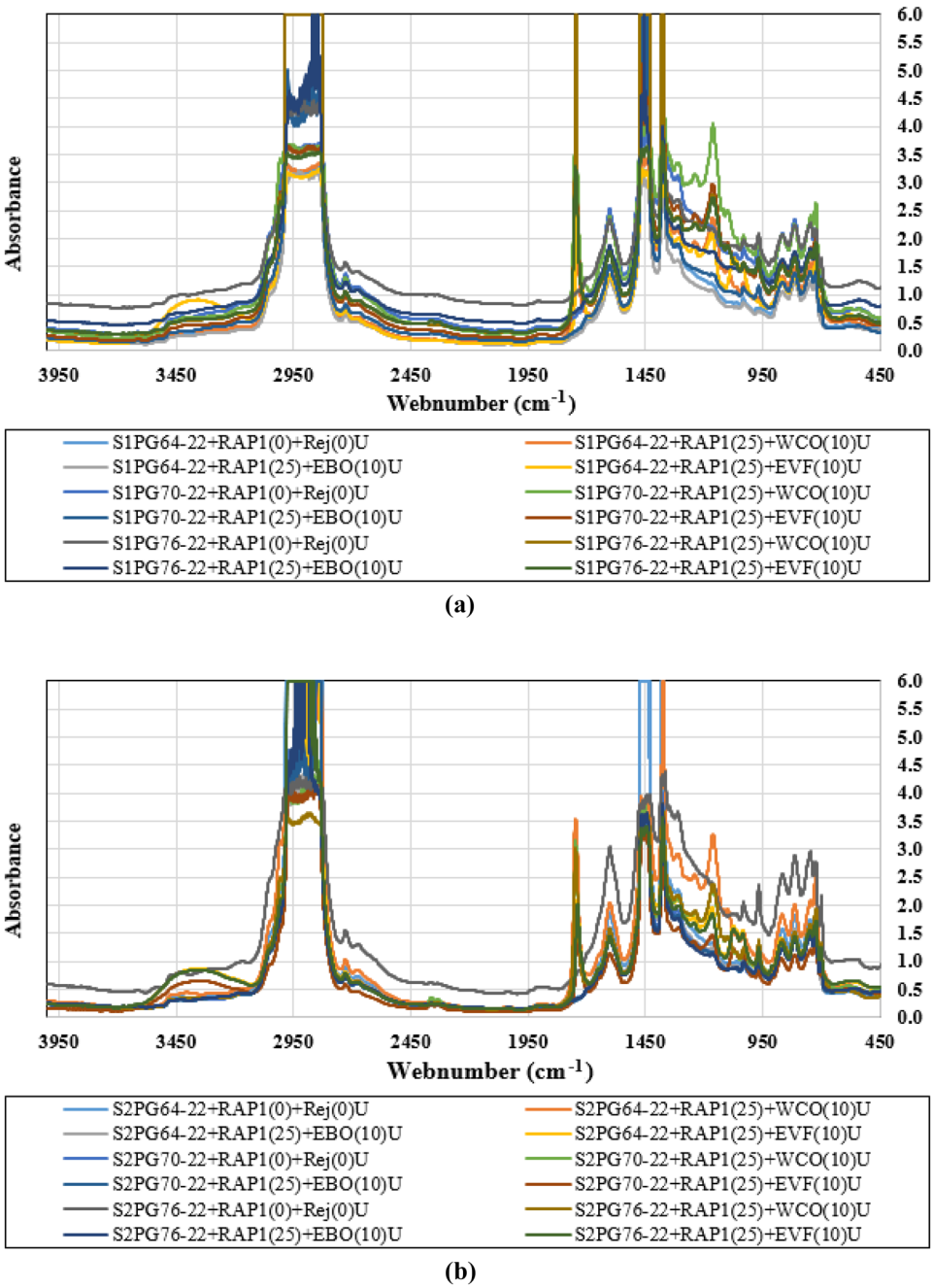

Fig. 8 FTIR spectra for rejuvenated binders from: **a** S1 and **b** S2, respectively

Trans-Butadiene index were quantitatively calculated using Eqs. (1), (2), and (3) [40, 41].

Carbonyl Index (C=O),

$$I_{C=O} = \frac{\text{Area of the Carbonyl band around } 1700\ \text{cm}^{-1}}{\text{Area of the spectral band between } 2000\ \text{cm}^{-1} \text{ and } 600\ \text{cm}^{-1}} \quad (1)$$

Sulphoxide-Index(S=O),

$$I_{C=O} = \frac{\text{Area of the Carbonyl band around } 1030\ \text{cm}^{-1}}{\text{Area of the spectral band between } 2000\ \text{cm}^{-1} \text{ and } 600\ \text{cm}^{-1}} \quad (2)$$

Trans-Butadiene Index (S=O),

$$I_{SBS} = \frac{\text{Area of the Carbonyl band around } 968\ \text{cm}^{-1}}{\text{Area of the spectral band between } 4000\ \text{cm}^{-1} \text{ and } 650\ \text{cm}^{-1}} \quad (3)$$

Table 6 represents the area under the curve corresponding to the specified three peaks and three indices were calculated using Eqs. (1), (2), and (3) for rejuvenated binders from S1 and S2. As seen in Table 6, the indices values are presented as italic form whereas the maximum increment in indices are shown in bold-italics. It is found that carbonyl index

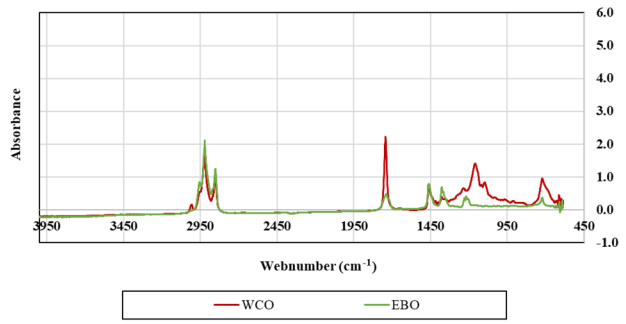

Fig. 9 FTIR spectra of WCO and EBO before using in RAP binder blends

was found to be increased for EVF-modified rejuvenated PG 64-22 (S1 and S2) and PG 76-22 (S2) binders; EBO-modified PG 70-22 (S1) and PG 76-22 (S2) binders; and WCO-modified PG 76-22 (S1) binder. It is also seen that the sulfoxide index was increased significantly with the addition of EBO in the case of PG 64-22 (S1 and S2) and PG 76-22 (S2) binders. The Trans-Butadiene index was also increased for EBO-modified PG 76-22 (S1) and PG 64-22 (S2) binders than the control binder. As seen in Fig. 9, these changes in the indices could have occurred due to the addition of WCO and EBO in the rejuvenated RAP binder blends. The FTIR spectra analyses of WCO and EBO softeners showed that there are distinct peaks observed between 4000 and 650 cm^{-1}. Therefore, it can be said that the appearance of these peaks can make changes in the peaks of the rejuvenated binders.

Table 6 Different indices obtained from the FTIR spectra for rejuvenated binders

Binder type	Total area (2000 cm^{-1} to 650 cm^{-1})	Wavenumber (1700 cm^{-1})		Wavenumber (1030 cm^{-1})		Wavenumber (968 cm^{-1})	
		Area	I (C=O)	Area	I (S=O)	Area	I (SBS)
PG 64-22 (S1)							
S1PG64-22+RAP1(0)+Rej(0)U	987	0.00	*0.0000*	2.22	*0.0022*	2.76	*0.0028*
S1PG64-22+RAP1(25)+WCO(10)U	1251	0.05	*0.0000*	3.70	*0.0030*	2.18	*0.0017*
S1PG64-22+RAP1(25)+EBO(10)U	858	1.58	*0.0018*	3.83	***0.0045***	2.20	*0.0026*
S1PG64-22+RAP1(25)+EVF(10)U	1106	48.08	***0.0435***	3.16	*0.0029*	0.18	*0.0002*
PG 70-22 (S1)							
S1PG70-22+RAP1(0)+Rej(0)U	1629	0.00	*0.0000*	3.53	*0.0022*	9.10	*0.0056*
S1PG70-22+RAP1(25)+WCO(10)U	1956	0.22	*0.0001*	3.87	*0.0020*	9.10	*0.0047*
S1PG70-22+RAP1(25)+EBO(10)U	1139	1.56	***0.0014***	2.44	*0.0021*	5.69	*0.0050*
S1PG70-22+RAP1(25)+EVF(10)U	1589	0.18	*0.0001*	3.83	***0.0024***	6.79	*0.0043*
PG 76-22 (S1)							
S1PG76-22+RAP1(0)+Rej(0)U	1169	0.00	*0.0000*	2.34	*0.0020*	6.53	*0.0056*
S1PG76-22+RAP1(25)+WCO(10)U	1416	44.99	***0.0318***	1.40	*0.0010*	5.81	*0.0041*
S1PG76-22+RAP1(25)+EBO(10)U	1092	0.54	*0.0005*	2.02	*0.0018*	6.24	***0.0057***
S1PG76-22+RAP1(25)+EVF(10)U	1411	0.28	*0.0002*	2.48	*0.0018*	2.11	*0.0015*
PG 64-22 (S2)							
S2PG64-22+RAP1(0)+Rej(0)U	1337	0.00	*0.0000*	4.69	*0.0035*	3.24	*0.0024*
S2PG64-22+RAP1(25)+WCO(10)U	1718	0.04	*0.0000*	5.01	*0.0029*	3.84	*0.0022*
S2PG64-22+RAP1(25)+EBO(10)U	1045	0.19	*0.0002*	4.00	***0.0038***	2.81	***0.0027***
S2PG64-22+RAP1(25)+EVF(10)U	1152	4.99	***0.0043***	1.51	*0.0013*	0.33	*0.0003*
PG 70-22 (S2)							
S2PG70-22+RAP1(0)+Rej(0)U	996	0.00	*0.0000*	2.91	*0.0029*	5.93	*0.0060*
S2PG70-22+RAP1(25)+WCO(10)U	1247	0.10	*0.0001*	3.23	*0.0026*	5.82	*0.0047*
S2PG70-22+RAP1(25)+EBO(10)U	971	0.51	*0.0005*	3.56	*0.0037*	5.33	*0.0055*
S2PG70-22+RAP1(25)+EVF(10)U	887	0.03	*0.0000*	2.64	*0.0030*	2.12	*0.0024*
PG 76-22 (S2)							
S2PG76-22+RAP1(0)+Rej(0)U	1738	0.00	*0.0000*	6.61	*0.0038*	14.24	*0.0082*
S2PG76-22+RAP1(25)+WCO(10)U	1319	0.12	*0.0001*	4.34	*0.0033*	8.25	*0.0063*
S2PG76-22+RAP1(25)+EBO(10)U	941	6.93	***0.0074***	4.22	***0.0045***	6.93	*0.0074*
S2PG76-22+RAP1(25)+EVF(10)U	1085	38.81	***0.0358***	4.02	*0.0037*	4.56	*0.0042*

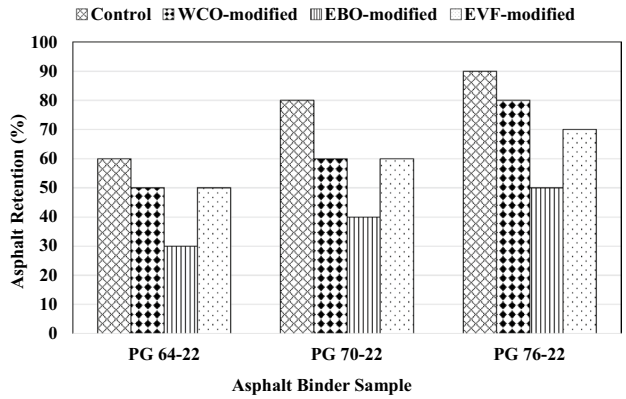

Fig. 10 TBT results of rejuvenated S1 binders

3.6 Boiling Tests (TBT)

Figure 10 shows the TBT results of the rejuvenated RAP blends from S1. In this test, the moisture damage potentials of the asphalt mixture were determined based on the percentage of the asphalt retention, through visual observation as per TTI guidelines. It was found that EBO-modified binders had a lower percentage of asphalt retention, irrespective of binder grades, among all rejuvenated binders used in this study. A similar percentage of asphalt retention was found for PG 64-22 and PG 70-22 binders in the case of WCO- and EVF-modified binder blends. For PG 76-22 binders modified with WCO showed a higher asphalt retention rate (80%) than EVF (70%). Based on the test results, it is evident that WCO can be effective in minimizing the moisture susceptibility of the asphalt mixtures and its TBT results are comparable with that of the engineered rejuvenator (EVF), especially for RAP-modified PG 64-22 and PG 70-22 binders.

4 Summary

The WCO increased the carbonyl index only for the PG 76-22 binder from Source 1. Based on the TBT results, the highest asphalt retention was observed for the WCO-modified PG 76-22 binder whereas EBO showed the lowest percentage of retention of asphalt binder among all rejuvenators regardless of the binders' grade.

5 Conclusions

The main goal of this study was to evaluate the efficacy of rejuvenated asphalt binders based on micro-mechanistic and spectroscopic techniques. Laboratory test results suggest that a 10% EBO or 10% WCO was effective in reducing the viscosity of the 25% RAP binder blends 'significantly, which in turn can reduce the mixing temperature up to 4 °C and compaction up to 12 °C. A reduction of DSR stiffness and an increase in the stress relaxation rate of rejuvenated RAP-blended binder indicate a reduction of fatigue and low temperature cracking potential in the pavement. The mano-level laboratory data of the rejuvenated binders are in agreement with the AFM-based nanomechanical properties such as modulus. The FTIR data confirmed the traces of EBO and WBO in the rejuvenated binder blends. Between WCO and EBO, WCO was found to be more effective against the stripping resistance of the rejuvenated RAP binder blends. Future research could be conducted to find the compositions of the WCO and EBO and their effects on asphalt binders' properties. Moreover, asphalt mixtures' performance tests could be incorporated into future studies.

Acknowledgements The authors acknowledge the financial support provided by the US Department of Transportation and the Arkansas Department of Transportation to conduct this study. The authors are thankful to the suppliers of asphalt binders, aggregates, and softening agents for their cooperation and support in providing test materials for this study. The authors are thankful to Dr. Syed Ashik Ali and Mr. Kenneth Hobson for their technical support in conducting the BBR tests. The authors are also thankful to Dr. Kotaiba for their technical support in conducting the FTIR tests. The authors are also thankful to the Arkansas Department of Transportation (ARDOT), Ergon, Inc., Marathon Petroleum, Paragon Testing Services, Atlas Paving, and other suppliers for providing test materials and technical support for this study.

Author contributions The authors confirm contribution to the paper as follows: study conception and design: ZH, SR; data collection: ZH, SR, GB, and MZ; analysis and interpretation of results: ZH, SR; draft manuscript preparation: ZH, and SR. All authors reviewed the results and approved the final version of the manuscript.

Funding The authors gratefully acknowledge the financial support provided by the National Science Foundation (CMMI: 1429690). The authors are also thankful to the suppliers of the materials for their technical support throughout this study.

Data availability The authors declare that the data supporting the findings of this study are available within the paper, and its supplementary information files.

Declarations

Conflict of interest We wish to confirm that there are no known conflicts of interest associated with this publication and there has been no significant financial support for this work that could have influenced its outcome.

References

1. Giustozzi, F., Crispino, M., Toraldo, E., & Mariani, E. (2015). Mix design of polymer-modified and fiber-reinforced warm-mix asphalts with high amount of reclaimed asphalt pavement: Achieving sustainable and high-performing pavements. *Transportation Research Record, 2523*(1), 3–10.
2. Copeland, A. (2011). *Reclaimed asphalt pavement in asphalt mixtures: State of the practice (No. FHWA-HRT-11-021)*. United

States. Federal Highway Administration. Office of Research, Development, and Technology.
3. Wright, Jr., F. (2001). *FHWA recycled materials policy*. Federal Highway Administration, Washington, DC. http://www.fhwa.dot.gov/legsregs/directives/policy/recmatpolicy.htm
4. Devulapalli, L., Kothandaraman, S., & Sarang, G. (2019). A review on the mechanisms involved in reclaimed asphalt pavement. *International Journal of Pavement Research and Technology, 12*, 185–196.
5. Cavalli, M. C., Partl, M. N., & Poulikakos, L. D. (2019). Effect of ageing on the microstructure of reclaimed asphalt binder with bio-based rejuvenators. *Road Materials and Pavement Design, 20*(7), 1683–1694.
6. Zaumanis, M., Mallick, R. B., Poulikakos, L., & Frank, R. (2014). Influence of six rejuvenators on the performance properties of reclaimed asphalt pavement (RAP) binder and 100% recycled asphalt mixtures. *Construction and Building Materials, 71*, 538–550.
7. Zhang, J., Zhang, X., Liang, M., Jiang, H., Wei, J., & Yao, Z. (2020). Influence of different rejuvenating agents on rheological behavior and dynamic response of recycled asphalt mixtures incorporating 60% RAP dosage. *Construction and Building Materials, 238*, 117778.
8. Mamun, A. A., & Al-Abdul Wahhab, H. I. (2020). Comparative laboratory evaluation of waste cooking oil rejuvenated asphalt concrete mixtures for high contents of reclaimed asphalt pavement. *International Journal of Pavement Engineering, 21*(11), 1297–1308.
9. Majidifard, H., Tabatabaee, N., & Buttlar, W. (2019). Investigating short-term and long-term binder performance of high-RAP mixtures containing waste cooking oil. *Journal of Traffic and Transportation Engineering (English Edition), 6*(4), 396–406.
10. Sun, D., Sun, G., Du, Y., Zhu, X., Lu, T., Pang, Q., Shi, S., & Dai, Z. (2017). Evaluation of optimized bio-asphalt containing high content waste cooking oil residues. *Fuel, 202*, 529–540.
11. Hugener, M., Partl, M. N., & Morant, M. (2014). Cold asphalt recycling with 100% reclaimed asphalt pavement and vegetable oil-based rejuvenators. *Road materials and pavement design, 15*(2), 239–258.
12. Chen, M., Xiao, F., Putman, B., Leng, B., & Wu, S. (2014). High temperature properties of rejuvenating recovered binder with rejuvenator, waste cooking and cotton seed oils. *Construction and Building Materials, 59*, 10–16.
13. Zaumanis, M., Mallick, R. B., & Frank, R. (2013). Evaluation of rejuvenator's effectiveness with conventional mix testing for 100% reclaimed Asphalt pavement mixtures. *Transportation Research Record, 2370*(1), 17–25.
14. Zargar, M., Ahmadinia, E., Asli, H., & Karim, M. R. (2012). Investigation of the possibility of using waste cooking oil as a rejuvenating agent for aged bitumen. *Journal of Hazardous Materials, 233*, 254–258.
15. Shen, J., Amirkhanian, S., & Tang, B. (2007). Effects of rejuvenator on performance-based properties of rejuvenated asphalt binder and mixtures. *Construction and Building Materials, 21*(5), 958–964.
16. Environmental Protection Agency (EPA). Online. *Managing, reusing, and recycling used oil*. Retrieved August 28, 2023, from https://www.epa.gov/recycle/managing-reusing-and-recycling-used-oil
17. Environmental Protection Agency (EPA), Online. *How much waste cooking oil is out there?* Retrieved from August 28, 2023, https://19january2017snapshot.epa.gov/www3/region9/waste/biodiesel/questions.html#howmuch
18. Bagchi, T., & Hossain, Z. (2021). Evaluation of compatibility of asphalt binders and aggregates. *Tran-SET 2020* (pp. 195–204). American Society of Civil Engineers.
19. Hossain, Z., Elsayed, A., Bagchi, T., & Roy, S. (2020). Assessment of compatibility of mineral aggregates and binders used in highway construction and maintenance projects. Tran-SET Project Number 19BASU02. Retrieved from https://repository.lsu.edu/transet_pubs/72
20. Rashid, F., Hossain, Z., & Bhasin, A. (2019). Nanomechanistic properties of reclaimed asphalt pavement modified asphalt binders using an atomic force microscope. *International Journal of Pavement Engineering, 20*(3), 357–365.
21. Jahangir, R., Little, D., & Bhasin, A. (2015). Evolution of asphalt binder microstructure due to tensile loading determined using AFM and image analysis techniques. *International Journal of Pavement Engineering, 16*(4), 337–349.
22. Nahar, S. N., Qiu, J., Schmets, A. J. M., Schlangen, E., Shirazi, M., Van de Ven, M. F. C., Schitter, G., & Scarpas, A. (2014). Turning back time: Rheological and microstructural assessment of rejuvenated bitumen. *Transportation Research Record, 2444*(1), 52–62.
23. Yu, X., Zaumanis, M., Dos Santos, S., & Poulikakos, L. D. (2014). Rheological, microscopic, and chemical characterization of the rejuvenating effect on asphalt binders. *Fuel, 135*, 162–171.
24. Nazzal, M. D., & Qtaish, L. A. (2013). *The use of atomic force microscopy to evaluate warm mix asphalt (No. FHWA/OH-2012/19)*. Ohio Department of Transportation.
25. Dourado, E. R., Simao, R. A., & Leite, L. F. M. (2012). Mechanical properties of asphalt binders evaluated by atomic force microscopy. *Journal of microscopy, 245*(2), 119–128.
26. Masson, J. F., Leblond, V., & Margeson, J. (2006). Bitumen morphologies by phase-detection atomic force microscopy. *Journal of Microscopy, 221*(1), 17–29.
27. Roy, S., & Hossain, Z. (2023). Effects of aging on multiscale mechanistic properties of asphalt binders. *International Journal of Pavement Research and Technology*. https://doi.org/10.1007/s42947-023-00333-8
28. Cavalli, M. C., Zaumanis, M., Mazza, E., Partl, M. N., & Poulikakos, L. D. (2018). Aging effect on rheology and cracking behaviour of reclaimed binder with bio-based rejuvenators. *Journal of Cleaner Production, 189*, 88–97.
29. Mokhtari, A., Lee, H. D., Williams, R. C., Guymon, C. A., Scholte, J. P., & Schram, S. (2017). A novel approach to evaluate fracture surfaces of aged and rejuvenator-restored asphalt using cryo-SEM and image analysis techniques. *Construction and Building Materials, 133*, 301–313.
30. Jia, X., Huang, B., Bowers, B. F., & Zhao, S. (2014). Infrared spectra and rheological properties of asphalt cement containing waste engine oil residues. *Construction and Building Materials, 50*, 683–691.
31. Hossain, Z., Lewis, S., Zaman, M., Buddhala, A., & O'Rear, E. (2013). Evaluation for warm-mix additive-modified asphalt binders using spectroscopy techniques. *Journal of Materials in Civil Engineering, 25*(2), 149–159.
32. Hossain, Z., Roy, S., & Rashid, F. (2020). Microscopic examination of rejuvenated binders with high reclaimed asphalts. *Construction and Building Materials, 257*, 119490.
33. Roy, S., & Hossain, Z. (2021). Use of molecular-level dissipated energy of asphalt binders to predict moisture effects on pavements. *International Journal of Pavement Engineering, 22*(11), 1351–1362.
34. Tarefder, R. A., & Zaman, A. M. (2010). Nanoscale evaluation of moisture damage in polymer modified asphalts. *Journal of Materials in Civil Engineering, 22*(7), 714–725.
35. Bagchi, T. (2020). *Evaluation of compatibility between asphalt binders and mineral aggregates*. Doctoral dissertation, Arkansas State University.

36. Bagchi, T., Hossain, Z., Ziaur Rahaman, M., & Baumgardner, G. (2021). Comparing Micro-and Macro-Level Rheological Properties of Polymeric and Reclaimed Asphalt Pavement-Modified Asphalt Binders. *Transportation Research Record*, *2675*(12), 247–263.
37. Roy, S., & Hossain, Z. (2019). Nanoscale quantification of moisture susceptibility of paving asphalts. In MATEC web of conferences (Vol. 271, p. 03005). EDP Sciences.
38. AASHTO T 312 (2008). Standard Method of Test for Preparing and Determining the Density of Hot Mix Asphalt (HMA) Specimens by Means of the Superpave Gyratory Compactor.
39. ASTM D2493/D2493M-16 (2017). Standard Practice for Viscosity-Temperature Chart for Asphalt Binders.
40. Liu, S., Peng, A., Wu, J., & Zhou, S. B. (2018). Waste engine oil influences on chemical and rheological properties of different asphalt binders. *Construction and Building Materials, 191*, 1210–1220.
41. Al Alam, M. S. (2017). *Chemical variations and engineering implications of reclaimed asphalt pavement and chemically modified asphalt binders*. Arkansas State University.

Springer Nature or its licensor (e.g. a society or other partner) holds exclusive rights to this article under a publishing agreement with the author(s) or other rightsholder(s); author self-archiving of the accepted manuscript version of this article is solely governed by the terms of such publishing agreement and applicable law.

Dr. Sumon Roy is a Staff Civil Engineer at Applied Research Associates, Inc. His research focuses on pavement engineering and pavement sustainability including pavement design, modification, and multiscale characterization of bituminous and recycled materials. He has experience in working as the lead researcher on several research projects funded by the United States Department of Transportation.

Dr. Zahid Hossain is a Professor of Civil Engineering at Arkansas State University. He has about 15 years of experience in developing sustainable transportation materials through mechanistic and surface science techniques. He has authored over 60 peer-reviewed articles and served as an Editor/Member of several scientific boards. Dr. Hossain is a registered Professional Engineer (PE) in the state of Arkansas.

Dr. Gaylon Baumgardner is Senior Vice President, Ergon Asphalt and Emulsions, Inc., a subsidiary of Ergon, Inc. of Jackson, MS, with thirty (30) plus years of experience in the petroleum and petroleum-related products industry. Under his direction, Paragon Technical Services, Inc., a division of Ergon Asphalt and Emulsions, Inc., is responsible for research and development services for Ergon Asphalt and Emulsions, Inc. and Ergon Armor, Inc. with primary focus in paving and related products, which include asphalt, polymer modified asphalt, asphalt emulsions, and polymer modified asphalt emulsions as well as specialty coatings.

Dr. Musharraf Zaman is a prolific teacher and a highly accomplished researcher. During his tenure at OU, he has received a number prestigious national-level teaching awards from the American Society of Engineering Education. He also received the lifelong title of David Ross Boyd Professorship, the highest teaching award given by the University of Oklahoma. During his tenure at OU, he has received over $14M in external funding from various state and federal agencies and industry. He has published over 200 archival papers. Several of his papers have won prestigious awards from national level societies and organizations.

Authors and Affiliations

Sumon Roy[1] · Zahid Hossain[2] · Gaylon Baumgardner[3] · Musharraf Zaman[4]

✉ Sumon Roy
sroy@ara.com

Zahid Hossain
mhossain@astate.edu

Gaylon Baumgardner
Gaylon.Baumgardner@ergon.com

Musharraf Zaman
zaman@ou.edu

[1] Applied Research Associates, Inc, 100 Trade Centre Drive, Suite 200, Champaign, IL 61820, USA

[2] Arkansas State University, LSW#246, PO Box 1740, Jonesboro, AR 72467, USA

[3] Paragon Technical Services, Inc., 390 Carrier Blvd, Richland, MS 39218, USA

[4] David Ross Boyd Professor and Aaron Alexander Professor of Civil Engineering, The University of Oklahoma, Norman, OK 73019, USA